THE ANALYST
FULL PAPER
www.rsc.org/analyst

# Chip-based refractive index detection using a single point evanescent wave probe

**Stephen C. Jakeway and Andrew J. de Mello***

*AstraZeneca/SmithKline Beecham Centre for Analytical Sciences, Imperial College of Science, Technology and Medicine, Department of Chemistry, South Kensington, London, UK SW7 2AY. E-mail: a.demello@ic.ac.uk*

***Received 17th May 2001, Accepted 29th June 2001***
***First published as an Advance Article on the web 16th August 2001***



This paper presents a novel approach for performing spectroscopic refractive index detection within microfluidic channel environments. Based on the principle of total internal reflection (TIR), changes in the refractive index of an analyte stream passing through a microfabricated channel are detected through interaction with an optical evanescent field formed at the channel wall. Refractive index variations within the microchannel environment modify the critical angle at the liquid–solid interface, thereby altering the characteristics of evanescent field formation in solution. These variations are evidenced through measurement of fluorescence intensities. Initially, the design and testing of the method are described. Subsequently, refractive index values for bulk sucrose solutions (0–35% w/v sucrose in water) are measured using the single point evanescent wave probe and compared with values obtained through conventional refractometry and the literature. Close agreement between all three approaches is demonstrated. The method is then applied to the detection of sucrose plugs (10–500 mM) hydrodynamically flowing through microfabricated channels on a planar glass chip. The evanescent wave probe is also used to selectively monitor specific analytes within a multicomponent system, by precise angular control in the vicinity of the critical angle. Although detection limits using the prototype system are non-ideal ($\sim$5 μM carbohydrate), they compare favourably with existing methods for on-chip refractive index detection.

## Introduction

Over the past decade, the development of miniaturised total analysis systems (μ-TAS) has seen an exponential growth. This has primarily been due to an emerging need for on-line measurements at low concentrations within the fields of DNA analysis, drug discovery, pharmaceutical screening, chemical production, medical diagnostics and environmental analysis.[1–5] In its true sense, a μ-TAS possesses many advantages with respect to its conventional (larger) analogues. These include improved efficiency with respect to sample size, response time, cost, throughput and automation. Indeed, the ultimate μ-TAS will include all steps of a complete analytical procedure (including sample handling, chemical reaction, sample pre-treatment, analytical separation, analyte detection and product isolation) on a single, integrated device.

It has long been understood that size limits for μ-TAS are primarily set by the system detector. Consequently, the adaptation of conventional detection methods to measurement in small volumes has closely accompanied the development of microfluidic devices for chemical analyses. To date, small-volume detection has generally focused on optical measurements. Of these, fluorescence techniques have proved particularly popular due to the inherent sensitivity and selectivity gains. Furthermore, most μ-TAS are conventionally fabricated from optically transparent materials, such as glass, quartz, polydimethylsiloxane and polymethylmethacrylate.[6] Consequently, detection limits for fluorescence-based measurements are extremely low, and as few as $10^5$ molecules are generally detectable in most laboratories utilizing laser-induced fluorescence (LIF) methods.[7] In addition, recent developments in the field of ultra-high sensitivity fluorescence detection have enabled single molecule detection to be routinely performed in planar chip devices.[8,9] Although fluorescence techniques are inherently sensitive, they are generally costly and not applicable for most molecular systems.

Accordingly, other approaches to 'on-chip' detection have been introduced and include electrochemiluminescence,[10] electrochemistry,[11] indirect fluorescence[12,13] and thermal conductivity methods.[14] More recently, the merging of electrospray ionization (ESI)-MS and microchips has allowed the analysis of extremely small samples at low flow rates (nL $min^{-1}$ to μL $min^{-1}$).[15–17] Since these flow rates closely match those encountered in many microfluidic chip systems, the ability to perform structural identification of analytes processed on μ-TAS devices has become a reality. For example, Karger and co-workers[18] demonstrated the first microfabricated glass chip coupled to ESI-MS. Peptide and protein samples were pumped by pressure and aligned by a precision translation stage to the MS inlet. In addition, Figeys and co-workers[19] have also used ion trap MS and ESI-MS with electro-osmotic pumping for the analysis of protein samples. Both approaches extend the applicability of μ-TAS to molecules that are non-fluorescent, and lead to the possibility of high-throughput MS analysis in screening and diagnostic applications.

The measurement of a change in refractive index (RI) has been successfully applied to many analytical techniques, including liquid chromatography and capillary electrophoresis. RI detection methods have useful characteristics that make them attractive alternatives to more conventional optical techniques. In particular, RI detection affords the generation of a signal for essentially all analytes. Furthermore, the analytical signal is concentration rather than mass sensitive and the technique is non-destructive.[20] Not surprisingly, researchers have endeavoured to develop methods for the measurement of RI variations in small volumes, with minimal background interferences.[21]

Although RI detectors have been commercially available for several years, it has only been recently that the RI detection methods have been applied to chip-based analysis devices. For example, Burggraf *et al.*[22] reported the application of a holographic forward scatter technique to a chip-based electrophoresis chip. Preliminary results demonstrated the feasibility

of using hologram-based RI detectors in microchip formats, although detection limits were poor (10 mM carbohydrate) in comparison with alternative methods. In addition, Bornhop and co-workers[23] have described elegant methods for the detection of RI variations in small volumes. For example, using micro-interferometric backscatter techniques, they were able to demonstrate submillimolar (743 μM) detection limits and sensitivities of approximately $10^{-6}$ RI units for a range of compounds. More recently, Ogita *et al.*[24] measured critical micelle concentrations (c.m.c.) in surfactant solutions by detecting adsorption onto an optical fibre. As surfactant adsorbs to the fibre, the RI in the surrounding surface of the core changes. The output signal suddenly increases at the c.m.c. due to a dramatic reflectivity change.

Unfortunately, many approaches to small-volume RI detection involve sophisticated optical instrumentation. This often complicates experimental design and subsequent integration with planar chip analysis devices. In this paper, we address this drawback and present a simple method to detect changes in RI within microfluidic channels. Based on the principle of total internal reflection, changes in the RI of an analyte stream passing through a microfabricated channel are detected through interaction with an optical evanescent field formed at the channel wall. The feasibility of the method is demonstrated for hydrodynamically flowing liquid streams.

## Theory

The behaviour of electromagnetic radiation when it encounters an interface between two dielectric media can be described according to Snell's law:

$$n_1 \sin\theta_1 = n_2 \sin\theta_2 \quad (1)$$

where $n_1$ is the RI of medium 1, $n_2$ is the RI of medium 2, $\theta_1$ is the angle of incidence (with respect to the normal) and $\theta_2$ is the angle of the transmitted ray (with respect to the normal). If light is travelling in the optically dense medium ($n_1$) and is incident at the interface at an angle less than a critical angle $\theta_c$, the incident beam will give rise to a reflected beam in medium 1 and a plane, transmitted wave in medium 2 (which is bent away from the normal). If $\theta_1$ is increased until it reaches $\sin^{-1}(n_2/n_1)$, the angle $\theta_2$ necessarily becomes $\pi/2$ rad and the transmitted wave travels along the interface. In this situation, the angle of incidence is termed the critical angle. If $\theta_1$ exceeds the critical angle, the existence of a propagating wave in medium 2 is formally forbidden and all the electromagnetic energy is reflected back into medium 1. This phenomenon is commonly termed total internal reflection (TIR).

However, if Maxwell's equations are solved for this type of dielectric system, it becomes apparent that a non-propagating electromagnetic field disturbance does exist in medium 2 in the vicinity of the boundary. This field is termed an evanescent wave. The properties of the evanescent wave can be calculated assuming that the electric field across the interface is continuous (the case for perpendicular polarized light is considered here). The boundary conditions for medium 1 and medium 2 mean that the intensity of the electromagnetic radiation at the interface, but in medium 2, is given by the following expression:

$$E_T = E_{0T} \exp -[(\omega^2/c^2)^{1/2} (n_2^2 - n_1^2 \sin^2\theta_1)^{1/2} x] \exp i(\omega t - k_{yi} y) \quad (2)$$

where $E_T$ is the electric field amplitude of the transmitted wave, $E_{0T}$ is the electric field amplitude of the transmitted wave at the interface, $\omega$ is the oscillation frequency of the wave, $c$ is the velocity of light in medium 1 and $x$ is the perpendicular distance away from the boundary (into medium 2). This expression demonstrates that the transmitted wave must decay exponentially with distance into the second medium, the first exponential describing the decay of the evanescent wave into the second medium and the second exponential describing the propagation of the electromagnetic component along the interface. As shown here, the evanescent wave is directly affected by the difference in the RI of the two media. Hence any change in this difference will cause a change in the evanescent wave. The variation of the onset of TIR (and thus evanescent wave formation) as a function of the RI of medium 2 is illustrated in Fig. 1. Here $\theta_c$ is plotted as a function of $n_2$ (where $n_1$ is fixed to be 1.467, the RI of fused silica). It can be seen that a small variation in $n_2$ (particularly when $n_2$ is similar in magnitude to $n_1$) leads to a large change in $\theta_c$.

Simplification of eqn. (2) yields:

$$E(x) = E_0 \exp - (x/d_p) \quad (3)$$

where $E(x)$ is the electric field amplitude of the evanescent wave at a given distance $x$, $E_0$ is the transmitted, interfacial electric field amplitude and $d_p$ is the depth of penetration. This term describes the distance at which the electric field amplitude has decayed to $e^{-1}$ of its interfacial value and is expressed by:

$$d_p = [\lambda_{vac}/(2\pi n_1)] \surd \{1/[\sin^2\theta_1 - (n_{21})^2]\} \quad (4)$$

where $\lambda_{vac}$ is the wavelength of the incident radiation *in vacuo*. Using this simple analysis of the boundary field, it is apparent that any change in the RI of medium 2 within a few micrometres of the channel wall will lead to a variation in both the characteristics of the evanescent wave and the onset of evanescent wave formation (or TIR). The variation of the onset of TIR, and thus the local RI in medium 2, will subsequently be evidenced by a change in the signal detected orthogonal to the interface.

## Experimental

### Reagents

All chemicals were purchased from BDH (Poole, UK) and used as provided unless otherwise specified. All aqueous solutions were made up using high-resistivity (18 MΩ) de-ionized water. A 500 mM stock solution of sucrose in 2 μM fluorescein (fluorescein disodium salt, Fluka, Poole, UK) was prepared and diluted with a 2 μM fluorescein solution to make subsequent solutions. Alternatively, for high w/v sucrose concentrations, solutions were made individually. Sucrose solutions without fluorescein were prepared in the same manner. Prior to use, the internal reflection element ($n$ = 1.467) was cleaned in 6% hydrogen peroxide–sulfuric acid (1 : 1) for 20 min at ambient temperature and then washed with copious amounts of water followed by hexane and methanol.

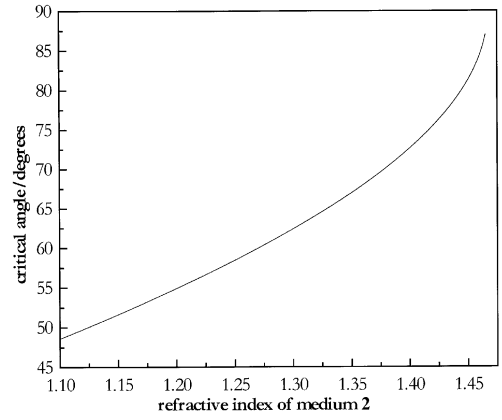


**Fig. 1** Variation of the critical angle as a function of the refractive index of medium 2. The refractive index of medium 1 is set to 1.467.

### Chip design and manufacture

Microfluidic channel patterns were designed using AutoCAD 2000©. Transparencies of the designs were created and used as masks in contact photolithography using a pre-coated substrate (100 nm low-reflectivity chrome, 0.5 μm AZ Photoresist; Nanofilm, Westlake Village, CA, USA). The channel design was transferred to the substrate by exposure to UV radiation (254 nm). Channels (200 μm wide by ~80 μm deep) were formed in the glass substrate using an etching solution (5% 7:1 $NH_4F$–HF, 9.25% HCl, in water). Removal of the exposed photoresist was achieved using a Microposit 351 developing solution (Shipley Europe Ltd, Coventry, UK). Removal of the chrome layer was achieved using a Chrome Etch Solution (Shipley Europe Ltd, Coventry, UK). Access holes (1.6 mm) were drilled through the substrate. The substrate and a glass cover plate were cleaned in HCl–MeOH (1:1) and $H_2SO_4$ before being thermally bonded in an oven. PTFE tubing (152 μm id, 1.6 mm od) was connected directly into chip reservoirs using epoxy resin.

### Instrumentation

A schematic diagram of the optical set-up is shown in Fig. 2. Details of the experimental set-up have been described previously elsewhere.[25] Briefly, excitation was provided by the 488 nm line from an argon ion laser (Lexel 95, Cooper LaserSonics Inc., Fremont, CA, USA). A 2.5 mm diameter beam was focused into the internal reflection element (IRE) using a 300 mm focal length lens (positioned so that the beam is at its narrowest when the incidence angle is closest to the critical angle). Computer control of the incidence angle was afforded using a rotating mirror mounted on a translation stage. An Immersol index matching oil ($n$ = 1.518; Carl Zeiss Ltd., Welwyn Garden City, UK) was used to interface the planar chip and the IRE.

Evanescent wave-induced fluorescence (EWIF) was focused onto the slits of a scanning, 0.22 m single monochromator (Spex 1881). Entrance and exit slits were set to produce a 10 nm bandpass. Fluorescence photons were detected using a single-photon counting system consisting of a photomultiplier tube (PMT) (Hamamatsu, R6358P) and a gated photon counter (Stanford Research Systems, SR400). By design, changes in the incidence angle were compensated for by changes in the optical path (*via* a translation stage) such that the position of the evanescent wave at the IRE–solution interface remained constant. The laser was attenuated with neutral density filters and a graded silver mirror as required. The signal from the PMT was displayed on a PC using a PCA III card and associated software (Oxford Instruments, Oakridge, USA).

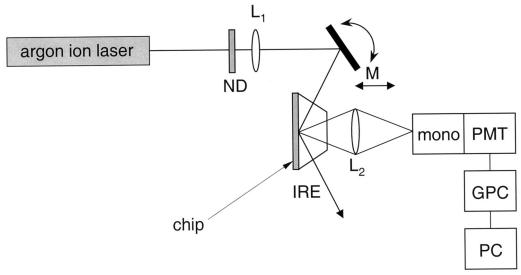


**Fig. 2** Schematic diagram of the instrumental layout used for evanescent wave probe measurements. Laser radiation is attenuated using a neutral density filter (ND) and focused through an internal reflection element (IRE) onto the chip using a 300 mm focal length lens ($L_1$). A rotating mirror (M) mounted on a translation stage provides control of both the point of total internal reflection (TIR) and the incidence angle. Fluorescence is collected using a condenser lens assembly ($L_2$) and focused onto the slits of a monochromator (mono) prior to detection by a photomultiplier tube (PMT) and a gated photon counter (GPC).

### Refractive index measurements

The RI of all solutions were measured on a standard laboratory refractometer (Abbe, Bellingham + Stanley, Tunbridge Wells, UK). For measurements using the EWIF system, a Teflon flow cell or microfluidic channel was filled with the desired solution. The cell and chip were rinsed several times with the desired solution prior to each measurement. The incidence angle was scanned from 75° to 65° and the fluorescence signal was measured. For repeat injection experiments, the chip was connected to a Rheodyne valve (7125, Alltech Associates, Carnforth, UK) with a 5.44 μL sample loop using 152 μm id PTFE tubing. Buffer solutions were pumped through the chip using a Harvard Apparatus pump (PHD 2000, Edenbridge, UK) at a rate of 10 μL $min^{-1}$. The sample loop was filled with the desired sucrose solution and the sample plug introduced onto the chip.

## Results

Accurate RI data for a diversity of liquids (both pure liquids and solutions) are available in reference tables. Furthermore, use of the general Lorentz–Lorenz formula allows the variation of RI with temperature to be predicted to within a few per cent.[26] Unfortunately, accurate theoretical predictions are difficult to achieve due to the fact that the RI is not simply dependent on the concentration and temperature.[21] Consequently, the validity of the proposed approach was tested by comparison with experimentally determined RI values.

The RI of eight solutions (0, 5, 10, 15, 20, 25, 30 and 35 w/v sucrose in water) were calculated using three different methods and the results are shown in Fig. 3(a). Here, literature RI values are compared with those measured on a standard laboratory refractometer and those calculated using the evanescent wave probe. For evanescent wave measurements, the critical angle of each sucrose solution was measured by calculating the angle at which the tangent at the point of inflection crosses the baseline [Fig. 3(b)]. Conversion of this angle into a measurement of RI is then achieved numerically using Snell's law.

Fig. 3(b) shows the dependence of the fluorescence intensity on the incidence angle for various concentrations of sucrose at a water–silica interface. For all measurements, fluorescein was present at a concentration of 2 μM to improve S/N. The large variation in the fluorescence intensity around the critical angle is due to the abrupt change from evanescent excitation to direct excitation as the angle of incidence decreases with respect to the normal. As can be seen, the change in the fluorescence signal occurs rapidly; with only a few hundredths of a degree variation causing a large change in the detector signal. Inspection of Fig. 3(a) demonstrates a close agreement between the RI values measured using both conventional refractometry and the EWIF probe. Furthermore, all experimentally determined RI values are in close agreement with accepted literature values.

The addition of fluorescein as a background fluorophore is well suited to an EWIF approach, since the change from evanescent excitation to direct excitation results in a large change in the optical path length (nm → μm) and thus in the observed fluorescence. Fluorescein was used in all experiments since its photophysical behaviour at a glass–water interface is well understood. In particular, Byrne *et al.*[25] demonstrated that the fluorescence quantum efficiency of fluorescein is unaffected by the presence of the glass–water interface. Indeed, analysis of the angle resolved EWIF profile of the 2 μM fluorescein solution [Fig. 3(b), curve a] confirms that the concentration distribution of fluorescein is homogeneous as a function of distance away from the interface.

Importantly, the described detection method is applicable to non-fluorescing systems, as shown in Fig. 3(c,d). Here, the RI of

sucrose solutions (0–30 w/v sucrose in water) were calculated using the previously defined techniques. Again, the agreement between the data obtained from conventional refractometry, the EWIF probe and the literature is good [Fig. 3(c)]. Inspection of Fig. 3(d) illustrates a significant reduction in S/N with respect to the data obtained with a background fluorophore in medium 2. This is due to the fact that the increased signal obtained from direct excitation (path length, ~80 μm) does not originate from fluorescein emission, but from low-level impurity emission and Raman scatter from the bulk solvent.

Subsequently, the EWIF methodology was applied to the analysis of dynamic RI variations within microchannel environments. Under hydrodynamic flow conditions, multiple 1 μL injections of 25 mM sucrose in 2 μM fluorescein were introduced into microfabricated channels (200 μm wide and 80 μm deep) under ambient conditions. To maximise the detection sensitivity, the incidence angle of the excitation beam was set to a few hundredths of a degree above the critical angle of the buffer system. This configuration ensures that any increase in the RI within the evanescent volume (in medium 2) will result in the destruction of TIR (through an increased critical angle) and thus direct excitation within the microchannel.

Fig. 4 illustrates the data resulting from four sequential, replicate injections of 25 mM sucrose in 2 μM fluorescein. The high reproducibility in peak shape and peak height (1.2% RSD) and the high S/N (~220) demonstrate the utility of the TIR geometry for the determination of intra-channel RI variations. Furthermore, the sensitivity afforded by the approach is equivalent to that achieved using previously reported methods.

The key to effective RI detection using TIR geometries is precise angular control in the vicinity of the critical angle. With the current instrumentation, the incidence angle of the excitation beam may be reproducibly varied in angular units of $1.75 \times 10^{-4}$ rad (0.01°). Furthermore, if the incidence angle is set marginally below the critical angle of the bulk solution, no analyte signal is observed, since evanescent wave formation is not achieved for the low RI limit. Consequently, a knowledge of the bulk solution RI is necessary when defining initial excitation conditions.

Fig. 5 illustrates similar data resulting from replicate injections of 25 mM sucrose in aqueous solution. Although of reduced intensity, analyte peaks were observable with a S/N of almost 60. Since the transition between TIR and direct excitation is governed by the relative ratio of the RI of medium 1 (fixed) and medium 2 (variable), careful choice of the incidence angle of the excitation beam allows selective control over analyte detection. In general, an incidence angle infinitesi-

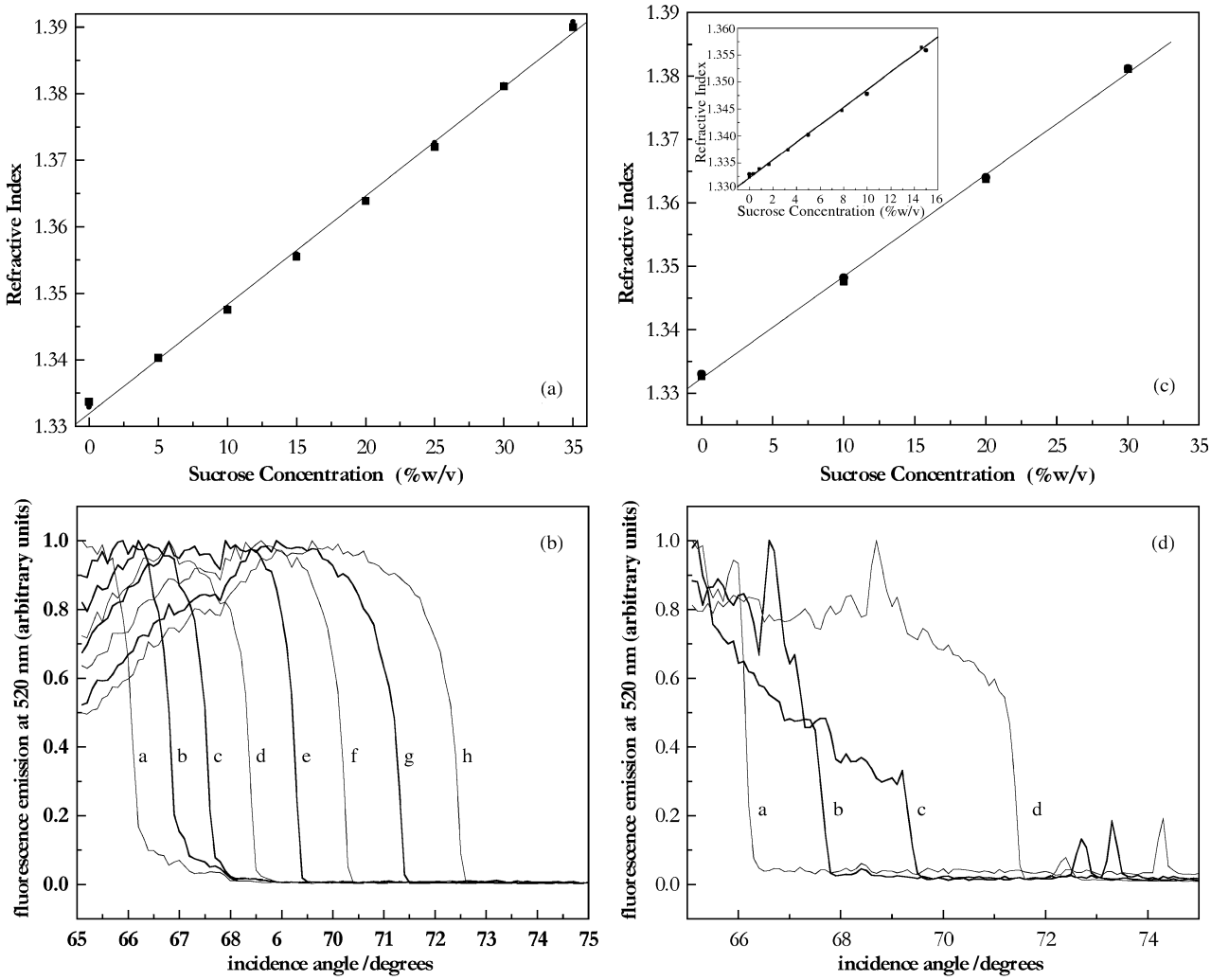


**Fig. 3** (a) Refractive indices of several aqueous sucrose solutions (in 2 μM fluorescein). The full line represents the refractive index values obtained from the literature. Experimental values were obtained using conventional refractometry (●) and the single point evanescent wave probe (■). (b) Angle resolved evanescent wave-induced fluorescence (EWIF) profiles of aqueous sucrose solutions (in 2 μM fluorescein) at a fused silica surface. Solution concentrations (w/v): a, water (control); b, 5% sucrose; c, 10% sucrose; d, 15% sucrose; e, 20% sucrose; f, 25% sucrose; g, 30% sucrose; h, 35% sucrose. (c) Refractive indices of several aqueous sucrose solutions. Legend as in (a). The inset shows additional measurements obtained for low sucrose concentrations. (d) Angle resolved EWIF profiles of aqueous sucrose solutions at a fused silica surface. Solution concentrations (w/v): a, water; b, 10% sucrose; c, 20% sucrose; d, 30% sucrose.

mally close, but greater than, the critical angle of the running buffer will allow any species with an RI greater than that of the buffer to be observed. However, if the incidence angle is set well in excess of the critical angle, species with RI close to that of the buffer will not be detected (since TIR will not be destroyed). Nevertheless, analytes with higher RI will be observed. For example, for the interface system used in the current studies (water–fused silica), an incidence angle 0.012 mrad above the critical angle will only allow analytes with a bulk RI in excess of 1.35 to be detected. This effect is illustrated in Fig. 6. Here, sequential injections of 500 and 250 mM sucrose solutions in 2 μM fluorescein are probed using an incidence angle of 68.00°. It can be observed that the higher concentration (and RI) analyte plugs are detected as expected but, since the incidence angle is now 33.2 mrad greater than $\theta_c$, the low RI analyte plugs are undetected. Consequently, this phenomenon can be used to selectively monitor specific analytes within a multicomponent system.

## Discussion

The studies presented herein describe the working principles of optical RI detection based on a single point evanescent wave probe. As such, the preliminary results demonstrate the feasibility of the approach for analyte detection within microfluidic chip devices. The analysis of a model disaccharide, such as sucrose, was chosen primarily for simplicity, but also as an example of an important class of macromolecules (carbohydrates) which are notoriously difficult to analyse using more conventional optical detection techniques. Since mono- and polysaccharides do not contain chromophores, direct quantitative analysis is not possible using UV absorption or fluorescence. Consequently, derivatization of carbohydrates using a variety of approaches (*e.g. via* reductive amination) has been a necessary extra step.[27] As stated, the most advantageous property of refractometry is its universal response. Analyte detection does not require the presence of a chromophore or fluorophore or any electrochemical activity, and is therefore well suited to high-efficiency carbohydrate analysis. Indeed, many commercial HPLC detectors for carbohydrate analysis are based on RI variation measurements.[23]

The application of RI variation measurements to miniaturised analysis systems (such as the microfluidic devices used in these studies) is particularly attractive for other reasons. First, as previously stated, refractometry is a concentration-dependent measurement. In other words, the analytical signal is independent of optical path length. This characteristic makes RI detection particularly desirable for probing ultra-small volumes (pL to nL range). Conversely, it is well known that small-volume absorption measurements are compromised due to the difficulty in probing small-volume cells, while maintaining a sufficiently long path length.[28] With microfabricated devices, this problem is exacerbated (due to reduced channel/capillary dimensions), and, to date, more restrictive fluorescence methods have proved to be far more useful.[6]

The primary drawback associated with RI measurements is the reduced sensitivity due to thermal fluctuations within the detection volume. The temperature dependence of the RI of aqueous systems is normally between $10^{-3}$ and $10^{-4}$ RI units $K^{-1}$ (this value can rise significantly for other solvent systems).[21] Since many applications require a sensitivity below $10^{-6}$ RI units, thermal stability becomes a dominant consideration in lowering detection limits. For example, in electrophoretic systems, buffer resistance to current transport causes Joule heating. Under high-field conditions, Joule heating can become so large as to cause intolerable band-broadening and electrolyte breakdown.[29] Furthermore, even moderate intracapillary heating will introduce temperature gradients within the capillary, thus dramatically diminishing the usefulness of RI detection in conventional formats. Fortunately, miniaturisation of channel dimensions both diminishes heat production and increases heat dissipation within the system (due to increased

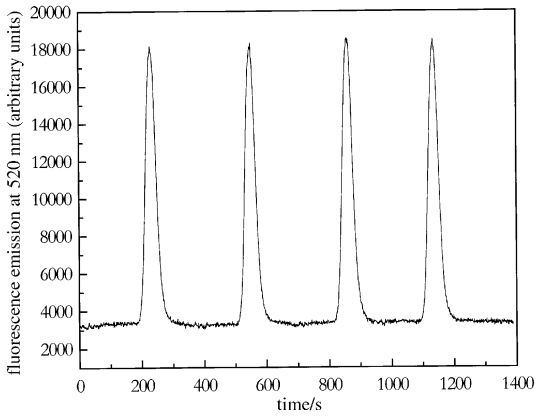


**Fig. 4** Replicate injections of aqueous sucrose solutions (in 2 μM fluorescein) monitored in a microfluidic channel using evanescent wave probe detection. Sucrose concentration, 25 mM; channel dimensions, 200 μm × 80 μm × 25 mm; running buffer, 2 μM aqueous fluorescein solution; $\theta_i$ = 66.25°.

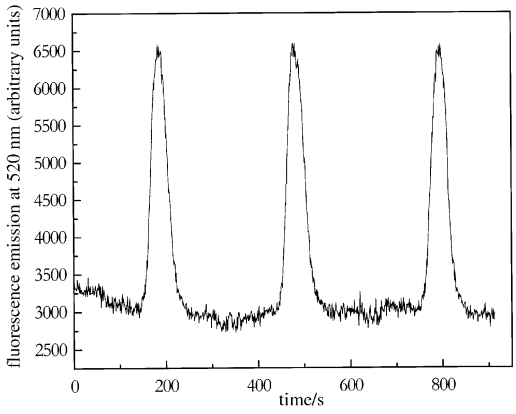


**Fig. 5** Replicate injections of aqueous sucrose solutions monitored in a microfluidic channel using evanescent wave probe detection. Sucrose concentration, 25 mM; channel dimensions, 200 μm × 80 μm × 25 mm; running buffer, water; $\theta_i$ = 65.88°.

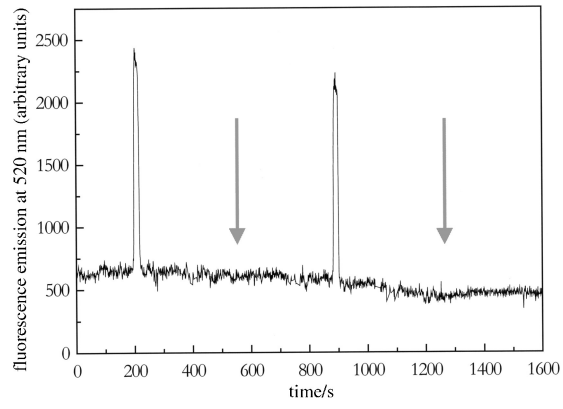


**Fig. 6** Sucrose injections monitored using evanescent wave probe detection. Alternate injections (1 μL) of 500 mM and 250 mM sucrose were performed at regular time intervals. 500 mM sucrose samples are observed at the expected times. Arrows indicate expected positions of the 250 mM sucrose samples. $\theta_i$ = 68.00°.

surface to volume ratios).[1] This, in turn, reduces intra-capillary temperature fluctuations and therefore associated noise in the RI signal. Furthermore, microfabricated channels most generally exhibit rectangular (or trapezoidal) cross-sections. This further increases surface to volume ratios and thus heat dissipation.

Finally, although RI detection has found uses in niche applications, its use in capillary HPLC has been limited by difficulties associated with integrating the detection system with conventional small-volume, fluid handling systems. By transferring these analytical technologies to planar chip formats, these problems are significantly reduced since optical interrogation is far simpler (*e.g.* optical interfaces are planar and parallel, and the chip footprint can be made very small).

The preliminary results presented in this paper demonstrate the utility of a single point evanescent wave as a probe of RI variations within microchannel environments. Limits of detection ($\sim$5 mM carbohydrate at S/N = 5) and sensitivity ($\Delta n \sim 5 \times 10^{-5}$ RI units) compare quite favourably with alternative RI protocols that have been used for on-chip analysis. The detection of sucrose plugs flowing hydrodynamically through microchannels was achieved with good reproducibility and sensitivity. Furthermore, the discriminatory power of the approach has been shown to allow for selective measurement of discrete components within a flowing stream. Current experiments have not explored the true potential of the detector for analysing low-concentration samples. Although far from ideal, current limits of detection are more than adequate for many kinds of routine carbohydrate analysis. Since RI variation measurements are concentration sensitive, the relative performance of the detector should improve when applied to analysis in small volumes (pL) with time constants of less than 10 ms. This fact implies that superior chip design will be the most obvious route to improved system performance. The simplicity of the single point evanescent wave probe is a major advantage with respect to other RI detection schemes. Due to the planar nature of most microfluidic chip devices, interrogation (*via* a single optical beam) is both simple and adaptable. Any location within the fluidic network is accessible without any variation in performance. Furthermore, the optical nature of the evanescent wave probe means that both conventional fluorescence and absorption measurements may be performed in tandem (allowing for variations in fluorescence quantum efficiencies near the channel walls).[30]

The studies presented herein are intended to be a first step towards a small-volume RI detector for chip-based analytical systems. Current investigations within our laboratories are now focusing on the assessment of the single point evanescent wave probe as a detection method for capillary electrophoresis (CE) carbohydrate separations on novel planar glass chips.

## Acknowledgements

The authors would like to thank EPSRC UK for financial support and SCJ acknowledges the receipt of an Overseas Research Studentship from the UK government. In addition, the authors are grateful to Dr J. de Mello and Dr E. Hill for useful discussions during the preparation of the manuscript.

## References

1 M. U. Kopp, H. J. Crabtree and A. Manz, *Curr. Opin. Chem. Biol.*, 1997, **1**, 410.
2 K. Schult, A. Katerkamp, D. Trau, F. Grawe, K. Cammann and M. Meusel, *Anal. Chem.*, 1999, **71**, 5430.
3 J. Wang, G. Rivas, X. Cai, E. Palecek, P. Nielsen, H. Shiraishi, N. Dontha, D. Luo, C. Parrado, M. Chicharro, P. A. M. Farias, F. S. Valera, D. H. Grant, M. Ozsoz and M. N. Flair, *Anal. Chim. Acta*, 1997, **347**, 1.
4 S.-H. Chen and J. M. Gallo, *Electrophoresis*, 1998, **19**, 2861.
5 J. Hicks, R&D Magazine Online, www.rdmag.com/features/features.htm, June 22, 1999
6 S. C. Jakeway, A. J. de Mello and E. L. Russell, *Fresenius' J. Anal. Chem.*, 2000, **366**, 525.
7 M. D. Barnes, W. B. Whitten and J. M. Ramsey, *Anal. Chem.*, 1995, **67**, A418
8 C. S. Effenhauser, G. J. M. Bruin, A. Paulus and M. Ehrat, *Anal. Chem.*, 1997, **69**, 3451.
9 B. B. Haab and R. A. Mathies, *Biophys. J.*, 1998, **74**, A9
10 A. Arora, A. J. de Mello and A. Manz, *Anal. Commun.*, 1997, **34**, 393.
11 A. T. Woolley, K. Lao, A. N. Glazer and R. A. Mathies, *Anal. Chem.*, 1998, **70**, 684.
12 N. J. Munro, Z. L. Huang, D. N. Finegold and J. P. Landers, *Anal. Chem.*, 2000, **72**, 2765.
13 S. Sirichai and A. J. de Mello, *Analyst*, 2000, **125**, 133.
14 S. C. Terry, J. H. Jerman and J. B. Angell, *IEEE Electron Device*, 1979, **26**, 1880.
15 M. C. Mitchell, V. Spikmans, A. Manz and A. J. de Mello, *J. Chem. Soc., Perkin Trans. 1*, 2001, 514.
16 M. C. Mitchell, V. Spikmans and A. J. de Mello, *Analyst*, 2001, **126**, 24.
17 F. Xiang, Y. Lin, J. Wen, D. W. Matson and R. D. Smith, *Anal. Chem.*, 1999, **71**, 1485.
18 Q. Xue, F. Foret, Y. M. Dunayevskiy, P. M. Zavracky, N. E. McGruer and B. L. Karger, *Anal. Chem.*, 1997, **69**, 426.
19 D. M. Pinto, Y. B. Ning and D. Figeys, *Electrophoresis*, 2000, **21**, 181.
20 K. Swinney, J. Pennington and D. J. Bornhop, *Microchem. J.*, 1999, **62**, 154.
21 A. Hanning and J. Roeraade, *Anal. Chem.*, 1997, **69**, 1496.
22 N. Burggraf, B. Krattiger, A. J. de Mello, N. F. de Rooij and A. Manz, *Analyst*, 1998, **123**, 1443.
23 K. Swinney, D. Markov and D. J. Bornhop, *Anal. Chem.*, 2000, **72**, 2690.
24 M. Ogita, Y. Nagai, M. A. Mehta and T. Fujinami, *Sens. Actuator B, Chem.*, 2000, **64**, 147.
25 C. D. Byrne, A. J. de Mello and W. L. Barnes, *J. Phys. Chem. B*, 1998, **102**, 10 326.
26 P. W. Atkins, *Molecular Quantum Mechanics*, Oxford University Press, Oxford, 2nd edn., 1983
27 E. K. Hill, A. J. de Mello, H. Birrell, J. Charlwood and P. Camilleri, *J. Chem. Soc., Perkin Trans. 2*, 1998, 2337.
28 H. Salimi-Moosavi, Y. T. Jiang, L. Lester, G. McKinnon and D. J. Harrison, *Electrophoresis*, 2000, **21**, 1291.
29 J. C. T. Eijkel, A. J. de Mello and A. Manz, *Organic Mesoscopic Chemistry*, ed. H. Masuhara and F. C. D. Schryver, Blackwell Science, Oxford, 1999, pp. 185–219
30 A. J. de Mello, B. Crystall and G. Rumbles, *J. Colloid Interface Sci.*, 1995, **169**, 161.